

Research Article

# Numerical Study of an Evaporative Exchanger Based on Fired Clay

Salifou Cisse<sup>1</sup>, Boureima Kabore<sup>1,2</sup>, Germain Wende Pouire Ouedraogo<sup>1,3</sup>, Sié Kam<sup>1,\*</sup>, Dieudonné Joseph Bathiebo<sup>1</sup>

<sup>1</sup>Laboratoire d'Energies Thermiques Renouvelables, Université Joseph KI-ZERBO, Ouagadougou, Burkina Faso

<sup>2</sup>Unité de Formation et de Recherche Sciences et Technologies, Université Norbert ZONGO, Koudougou, Burkina Faso

<sup>3</sup>Ecole Supérieure d'Ingénierie (ESI), Université de Fada N'Gourma, Fada N'Gourma, Burkina Faso

## Abstract

Evaporative air coolers are one of the alternatives to conventional air conditioners for cooling the air in the building. These systems consume less energy and contribute to the reduction of greenhouse gases. This work is a numerical study of an evaporative exchanger based on fired clay plates using COMSOL Multiphysics software. It was interested in hygrothermal transfers for air cooling. This study allowed to highlight the impact of the gap between the fired clay plates, the speed of the area as well as the air temperature at the inlet of the exchanger on the evolution of temperature and relative humidity of the air along the fired porous clay plates. The thermal efficiency of the exchanger was subsequently evaluated. This study allowed to note that there is a drop of 14 K along the porous plates of fired clay. Speed has an influence on outlet temperatures and relative humidity. For a speed of 0.2m/s, the temperature variation is 16 K and for speeds ranging from 2 m/s to 4m/s, the temperature variations are approximately 17 K. For gaps in porous plates of fired clay less than 2cm, the thermal efficiency varies 92% to 98%.

## Keywords

Exchanger, Evaporation, Fired Clay, Hygrothermal Transfers

## 1. Introduction

Air conditioning is a major energy issue in premises with the increase in populations and the urbanization of urban centers [1]. Indeed, urban centers are warmer because the buildings house more people; Household appliances, including conventional air conditioning systems, generate heat by consuming a lot of electricity. The air conditioning technique using evaporative exchangers can be an alternative to refrigeration systems for air cooling in buildings [2]. An evaporative exchanger or evaporative cooler is an exchanger that

cools air by evaporating water [3]. Evaporative cooling uses the fact that water absorbs a relatively large amount of heat from hot, dry air to evaporate [4]. The objective of this work is to carry out a numerical study of hygrothermal transfers in an evaporative exchanger for air cooling in a hot and dry climate. Transfer modules in a porous medium from COMSOL Multiphysics is used. COMSOL Multiphysics is an advanced software for the modeling and simulation of physical phenomena described by systems of partial differential

\*Corresponding author: [kamsie75@gmail.com](mailto:kamsie75@gmail.com) (Sié Kam)

**Received:** 8 February 2024; **Accepted:** 27 February 2024; **Published:** 13 March 2024



equations (PDE) solved by finite elements [5].

## 2. Methodology

### 2.1. Operating Principle of the Evaporative Exchanger

The cooling mechanism is based on heat and mass transfers resulting from the evaporation of water through a porous wall, particularly fired clay. By forced convection, hot ambient air is circulated between plates of fired clay placed vertically. A device placed above the system allows water to flow by drops onto the plates. Thus, the plates placed vertically remain permanently soaked in water. Water infiltrates the porous plates by capillary action without reaching the state of saturation. The passage of hot, dry air over these plates, which are permanently soaked in water, causes the water to evaporate and the air becomes charged with humidity. The air gives up its sensible heat to the water which evaporates and in return receives the latent heat resulting from evaporation [4]. A lower air temperature at the outlet of the device is therefore obtained.

### 2.2. Description of the Prototype

The prototype studied is a cubic shell heat exchanger inside which fired clay plates are placed. The plates numbering two (2) inside the exchanger are arranged parallel. Two recesses on two opposite sides of the PVC grille allow the entry and exit of air from the exchanger. A device placed above the system allows the fired clay plates to be permanently soaked in water. And a fan blows hot, dry air into a hollow in the tank. The air is then cooled by evaporation. The schematic diagram and dimensions of the device used for the study are presented respectively in Figure 1 and Table 1.

**Table 1.** Dimensions of the device used for the study.

Module length	$L_{mod} = 20 \text{ cm}$
Module width	$l_{mod} = 20 \text{ cm}$
Length of clay plates	$L_{plaque} = 18 \text{ cm}$
Width of clay plates	$l_{plaque} = 18 \text{ cm}$
Plate thickness	$e_{plaque} = 18 \text{ cm}$
Gap between plates	$Ec_{plaque} = 2 \text{ cm}$
Distance between PVC wall plate	4.1cm
Number of plates	3
Air duct section	$36 \text{ cm}^2$
Air duct perimeter	40 cm

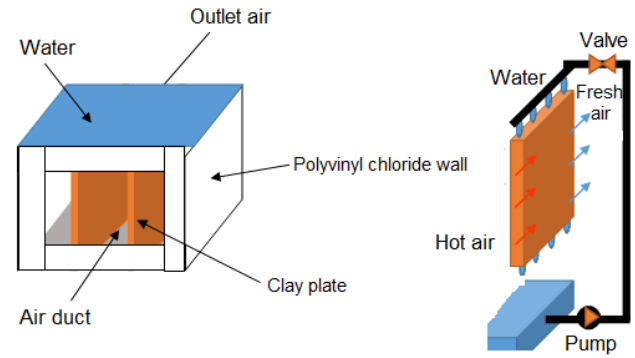


**Figure 1.** Schematic diagram of the evaporative exchanger.

## 3. Mathematical Model

### 3.1. Simplifying Assumptions

- 1) Transfers are considered one-dimensional in the radial direction. These hypotheses make it possible to take into account two types of heat transfer: Sensible heat transfer and latent heat transfer resulting from mass transfer by evaporation;
- 2) The overall heat exchange coefficient is constant;
- 3) The fluid temperature is constant across a cross section;
- 4) The mass flow rates of the two fluids are constant;
- 5) The specific heats of the two fluids are constant;
- 6) The physical characteristics of the materials are constant throughout the exchanger.

### 3.2. Heat Transfer

In general, the instantaneous variation of the energy rate in an element ( $i$ ) of a system is the algebraic sum of the flux densities exchanged within this element ( $i$ ) [6].

$$M_i C_{pi} \frac{dT_i}{dt} = FSA_i + Q_{mi} + \sum_j \sum_x h_{xji} (T_j - T_i) \quad (1)$$

$M_i, C_{pi}, T_i$  and  $T_j$  are respectively the mass ( $kg$ ), the specific heat ( $J.kg^{-1}.K^{-1}$ ), the temperature ( $K$ ) of the element ( $i$ ) and the temperature ( $K$ ) exchanged with ( $i$ ).

$FSA_i$ : Solar flux absorbed by ( $i$ ) in  $W$ .

### 3.3. Mass Transfer

The equation for mass transfer by convection between the saturated vapor at the water interface - wall of the porous plates and the ambient air by analogy with Newton's equation in heat transfer by convection, is written [7]:

$$\dot{m}_{ex} = K_c S (C_{vsat} - C_{va}) \quad (2)$$

$C_{vsat}$ : Saturating vapor concentration

$C_{va}$ : Vapor concentration in air

$K_c$ : Mass transfer coefficient

and the mass flux per unit area is given by equation (3)

$$d\dot{m}_{ex} = K_c dS (C_{vsat} - C_{va}) \quad (3)$$

Assuming that air and water vapor are ideal gases, the following equation is obtained:

$$C_{va} = \frac{P_{va}}{R_v T} \quad (4)$$

And

$$C_{vsat} = \frac{P_{vsat}}{R_v T} \quad (5)$$

From where:

$$d\dot{m}_{ex} = \frac{K_c dS}{R_v T} \left[ P_{vsat} (T_{eau\_splaq}) - P_{vair} (T_{air}) \right] \quad (6)$$

- $dS$ : Surface following a slice  $dx$  ( $m^2$ );
- $R_v$ : Water vapor constant ( $J/mol.K$ );
- $P_{vsat}$ : Saturating vapor pressure ( $P_a$ );
- $P_{vair}$ : Vapor pressure in air ( $P_a$ ).

### 3.4. Energy Balance of the System

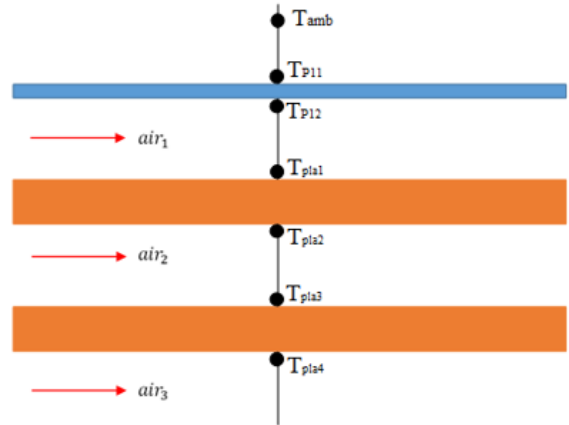


Figure 2. Diagram of a horizontal view of the system.

The energy balance will concern the humidified porous plates, the air circulating between the plates as well as the PVC. Figure 2 gives an overview of the energy balance seen horizontally.

The system is devised into successive slices with variable average temperature  $T_i$ . From one section to another the energy balance in these sections is applied.

$$\frac{M_{pvc}}{2} C_{pvc} \frac{dT_{p11}}{dt} = -h_{dpvc} ds (T_{p11} - T_{p12}) + h_{ca} ds (T_{amb} - T_{p11}) \quad (7)$$

$$\frac{M_{pvc}}{2} C_{pvc} \frac{dT_{p11}}{dt} = h_{dp} ds (T_{p11} - T_{p12}) + h_{ca} ds (T_{air_1} - T_{p12}) \quad (8)$$

$$G_a (C_{pas} + W \cdot C_{pe}) dT_{air_1} = -h_{ca} ds (T_{air_1} - T_{pla_1}) - h_{ca} ds (T_{air_1} - T_{p12}) \quad (9)$$

$$\frac{M_p}{2} C_{pp} \frac{dT_{pla_1}}{dt} = -h_{dp} ds (T_{pla_1} - T_{pla_2}) + h_{ca} ds (T_{air_1} - T_{pla_1}) - \dot{m}_e L_v \quad (10)$$

$$\frac{M_p}{2} C_{pp} \frac{dT_{pla_1}}{dt} = h_{dp} ds (T_{pla_1} - T_{pla_2}) + h_{ca} ds (T_{air_2} - T_{pla_2}) - \dot{m}_e L_v \quad (11)$$

$$G_a (C_{pas} + W \cdot C_{pe}) dT_{air_2} = -h_{ca} ds (T_{air_2} - T_{pla_2}) - h_{ca} ds (T_{air_2} - T_{pla_3}) \quad (12)$$

$$\frac{M_p}{2} C_{pp} \frac{dT_{pla_3}}{dt} = -h_{dp} ds (T_{pla_3} - T_{pla_4}) - h_{ca} ds (T_{pla_3} - T_{air_2}) - \dot{m}_e L_v \quad (13)$$

$$\frac{M_p}{2} C_{pp} \frac{dT_{pla_4}}{dt} = h_{dp} ds (T_{pla_4} - T_{pla_3}) + h_{ca} ds (T_{air_3} - T_{pla_4}) - \dot{m}_e L_v \quad (14)$$

$$G_a (C_{pas} + W \cdot C_{pe}) dT_{air_3} = -h_{ca} ds (T_{air_3} - T_{pla_4}) - h_{ca} ds (T_{air_3} - T_{pla_5}) \quad (15)$$

### 3.5. Determination of Parameters

In order to solve the equations listed above, the heat transfer coefficients will be determinate. And this using the relationships from the literature best suited to the problem.

- a) Natural convection of ambient air on the PVC surface  
The coefficient of convection of the ambient air on the

PVC walls due to the wind is given by equation (16) which is an empirical equation [8]:

$$h_{cae} = 2,8 + 3,3 \quad (16)$$

$V_{cae}$  represents the wind speed in  $m \cdot s^{-1}$ .

b) Conduction coefficients

Conduction coefficient of PVC: in PVC the conduction

coefficient is given by equation (17):

$$h_{dpvc} = \frac{\lambda_{pvc}}{e_{pvc}} \quad (17)$$

With:  $\lambda_{pvc}$ , the thermal conductivity of PVC;  $e_{pvc}$ , the thickness of the PVC.

Conduction coefficient of porous plates: the conduction coefficient of the porous plate is given by equation (18):

$$h_{dp} = \frac{\lambda_p}{e_p} \quad (18)$$

With:  $\lambda_p$  and  $e_p$ , respectively the thermal conductivity and the thickness of the plate.

c) Radiation coefficient on PVC surface

The radiation on the surface of the PVC is due to the celestial vault. The exchange radiation coefficient is given by equation (19):

$$h_{rvs} = \varepsilon_{pvc} \sigma (T_{pvc}^2 + T_{vs}^2) (T_{pvc} + T_{vs}) \quad (19)$$

Or:  $\sigma = 5,671 \cdot 10^{-8} W \cdot m^{-2} \cdot K^{-4}$ , the Stefan-Boltzmann constant;  $T_{pvc}$ , the temperature of the PVC;  $\varepsilon_{pvc} = 0,94$ , the emissivity of PVC.

The temperature of the celestial vault is given by the S win bank formula by equation (20):

$$T_{vc} = 0,0552 \times T_{amb}^{1,5} \quad (20)$$

With  $T_{amb}$  the ambient air temperature.

d) Air flow

The mass flow rate of air following a section (i) causing water evaporation is given by equation (21).

$$Ga = \rho \cdot V_{air} \cdot S_i \quad (21)$$

$V_{air}$ , air speed in  $m \cdot s^{-1}$ ;  $S_i$ , air pass section in  $m^2$ .

### 3.6. Boundary Conditions and Initial Conditions

A heat flow is subjected to the exchanger surface to approximate physical reality.

Conditions to the limits:  $\lambda_m \frac{\partial T}{\partial x} \Big|_0 = h_a S_i (T_f - T_a) - \dot{m}_e L_f$

Initial condition:  $t=0; T_e = T_p$  And  $T_a = T_{amb}$

Figure 3 gives us the distribution of initial temperatures in the exchanger

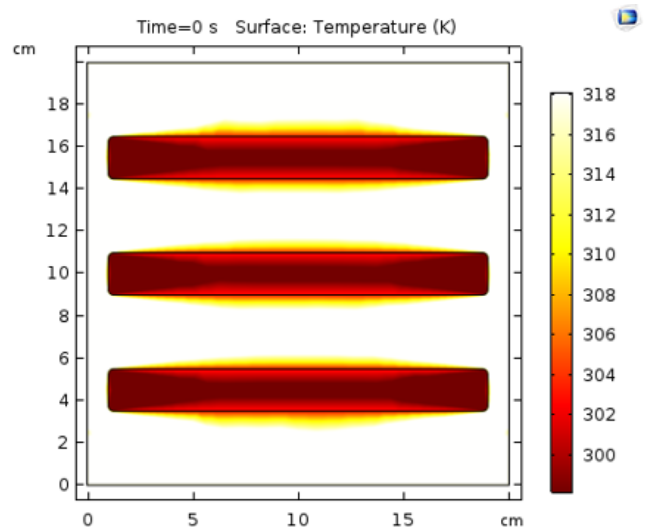


Figure 3. Initial conditions in the exchanger.

### 3.7. Physical Properties and Input Parameters

The properties of fired clay, PVC, air and water are given in table 2.

Table 2. Physical properties of fired clay, PVC, air and water [9-13].

Properties	Cooked clay	PVC	Air	Water
Thermal conductivity ( $W \cdot K^{-1} \cdot m^{-1}$ )	0.6	0.18	0.026	0.59
Specific heat ( $J \cdot Kg^{-1} \cdot K^{-1}$ )	850	1470	1000	4185
Volumic mass ( $kg \cdot m^{-3}$ )	1380	1190	1250	1000
Dynamic viscosity (Pa.s)	-	-	$168,2 \cdot 10^{-8}$	$547,1 \cdot 10^{-8}$
Porosity (%)	0.3	-	-	-

Table 3 gives the input parameters for the simulation of hydrothermal transfers in the exchanger.

**Table 3.** Input parameters for simulation.

Arete of the tank (PVC) of the exchanger (cm)	20
Baked clay arete (cm)	18
Thickness of fired clay (cm)	2
Air inlet temperature (K)	318.15
Air speed (m/s)	1
Water inlet temperature (K)	298.15
Temperature of fired clay (K)	300.15

### 3.8. Solver Parameters

The heat transfer model in porous media was used to model heat and mass transfer in porous plates. Convection is forced. Radiation heat transfer model was used on the upper side of PVC. The analysis is temporal and the resolution time is 15 min (900 s) with a time step of 5 s. The relative tolerance is 0.01 for all parameters. The discretization used is of the Lagrange-linear type (Finite Element Method).

## 4. Results and Analysis

### - Isothermal surfaces or temperature surfaces

The isothermal surfaces make it possible to determine the temperatures at any point of the exchanger. These surfaces are shown in Figure 4.

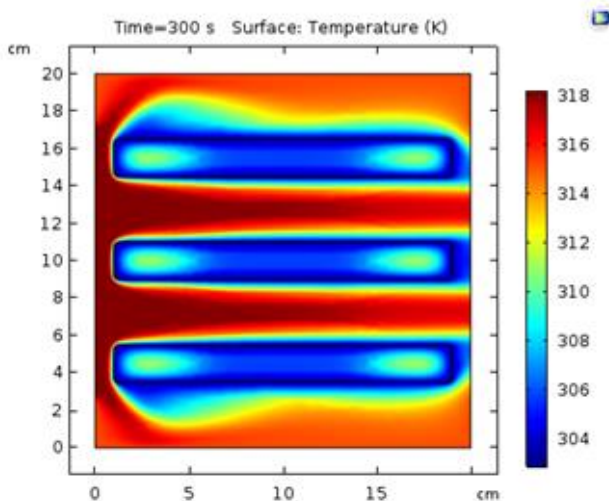


**Figure 4.** Temperature surfaces.

We observe in Figure 4 that the strong temperature variations from 318K to around 300K take place close, around 7mm, to the surface of the wet porous plates. The colors blue, green and yellow indicate vapor diffusion in the air. The blue color indicates greater diffusion of vapor in the air because it is closer to wet porous plates. This vapor transmitted to the

air comes from the evaporation of water. Water captures sensible heat from the air as it evaporates and gives up its latent heat. The maximum temperature is noted at the entrance to the exchanger and is 317.5K. There is a significant decrease in air temperature of 292.15K as it passes the surface of the plates.

### - Evolution of the air temperature between the exchanger plates

The curves in Figure 5 shows the evolution of the air temperature in the exchanger for a spacing between the fired clay plates of 5cm, 4cm, 3cm and 2cm.

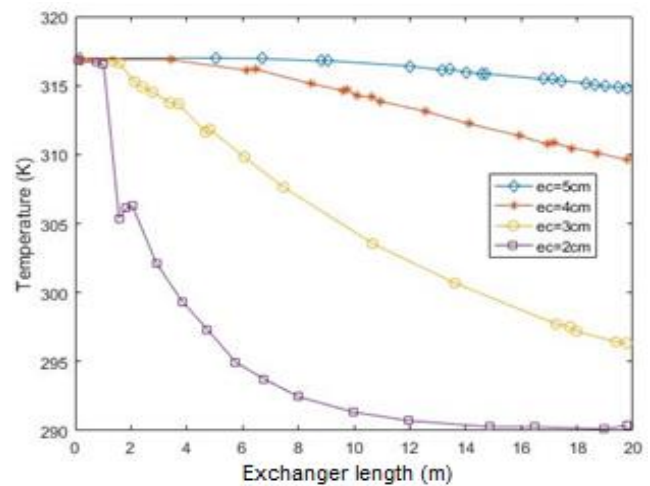


**Figure 5.** Evolution of air temperature for different spacing of porous plates.

Figure 5 show that whatever the gap between the porous plates, there is a drop in the air temperature from the inlet to the outlet of the exchanger. It is also observed that when the gap between the porous plates decreases, the temperature drop is significant. There is a significant reduction in air temperature at position 0 to 10 cm along the exchanger.

The largest temperature difference (25 K) is observed with a 2 cm difference in the porous plates. These results show that the walls of the plates soaked in water have an influence on the thermal exchanges between the air and the water.

Subsequently, the evolution of the air temperature for different air speeds is studied. The gap between the porous plates is 2 cm. Figure 6 gives the evolution of the temperature for different air speeds.

Figure 6 show that when the air speed increases, its temperature at the outlet of the exchanger decreases. The air temperature decreases regardless of the inlet air speed. Analysis of the curves shows that with an air speed ranging from 0.2 m/s to 4 m/s, sudden temperature drops of around 16 K over a distance of 6 cm in the exchanger is observed. From this position, a stabilization, around 301 K, of the air temperature is observed.

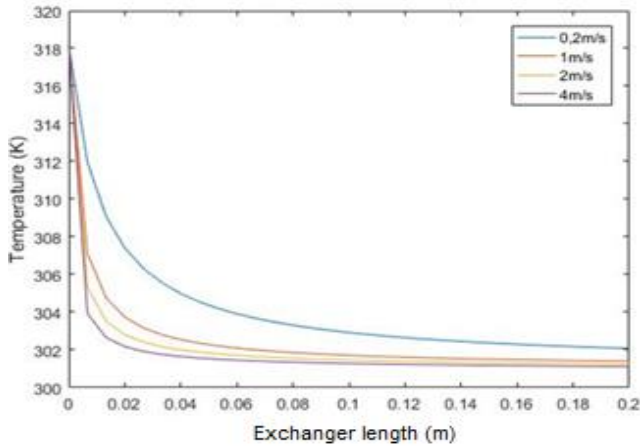


Figure 6. Evolution of air temperature for different inlet speeds.

Thus, the increase in air speed leads to an increase in convective air exchanges. This trend is no longer a reality if the air speed exceeds 4 m/s. Since the air no longer has the time necessary to exchange heat with the porous plates.

In conclusion, for good heat exchange efficiency, the optimal air speed must be around 4 m/s.

To properly study the heat and mass transfers in the exchanger leading to the cooling of the air, it is necessary to vary the temperature of the air at the inlet of the exchanger. Figure 7 gives the influence of the air inlet temperature in the exchanger on heat and mass transfers.

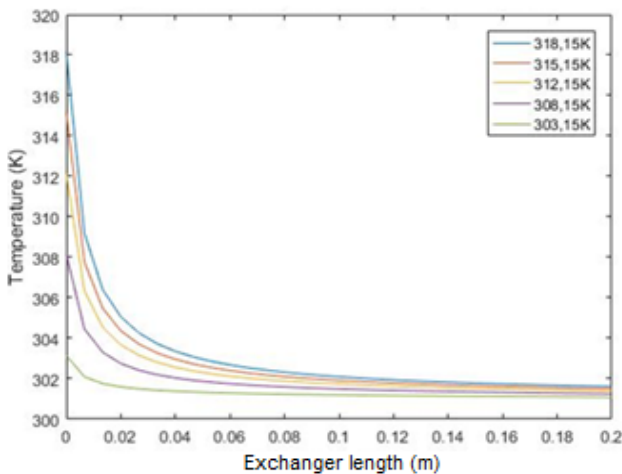


Figure 7. Evolution of the air temperature in the exchanger as a function of the air inlet temperature.

Figure 7 show that whatever the temperature at the inlet of the exchanger, there is a sudden drop in temperature of around 14 K, to reach stability from position 0.06 m.

For air inlet temperatures of 318.15; 315.15; 312.15; 308.15; 303.15 K the air temperature at the outlet of the exchanger is approximately 301.5 K. There is therefore a convergence of temperatures at the outlet of the exchanger.

1) Evolution of relative humidity in the exchanger

The relative humidity curves for temperatures of 318.15K, 315.15K and 308.1K of the air at the changer inlet with respective initial relative humidities of 30%; 35% and 40% are shown in Figure 8.

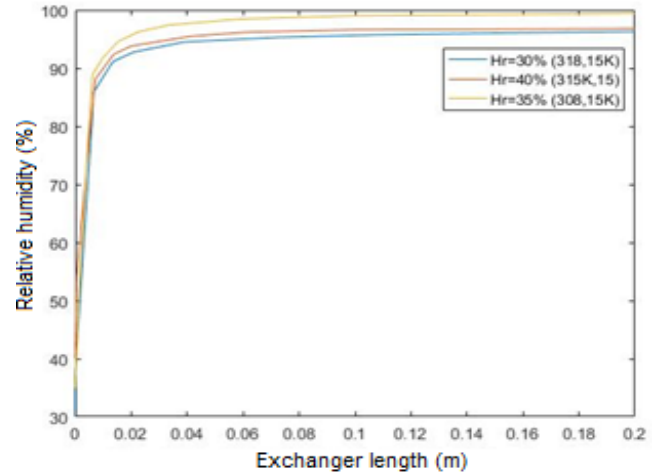


Figure 8. Evolution of relative humidity in the exchanger for different initial values of relative humidity.

The curves in Figure 8 show the variation of relative humidity in the exchanger for different initial values of relative humidity linked to different temperatures. The maximum relative humidity is 98% for a pair of temperature and initial relative humidity (315.15 K, 35%) are noted. For couples (318.15 K, 30%) and (308.15 K, 40%) of the air, a relative humidity of approximately 96% at the outlet of the exchanger is obtained. This increase in the relative humidity of the air at the outlet of the exchanger is always observed.

2) Thermal efficiency of the evaporative exchanger

The thermal efficiency of an exchanger allows to know its thermal performance. Its expression is given by equation (22). [14]

$$\varepsilon = \frac{T_e - T_s}{T_e - T_h} \tag{22}$$

With:  $T_e$ : air inlet temperature;  $T_s$ : air outlet ture;  $T_h$ : wet bulb temperature.

Figure 9 shows the evolution of the thermal efficiency of the exchanger along the porous plates for different air speeds.

When air inlet speed the 0,2 m/s thermal efficiency is 94%. For an air inlet speed the 4 m/s thermal efficiency is approximately 98%. The thermal efficiency of the exchanger increases with the speed of air entry into the exchanger. In addition, when air is in contact with wet porous plates, thermal efficiency increases. The exchanger is efficient for air cooling.

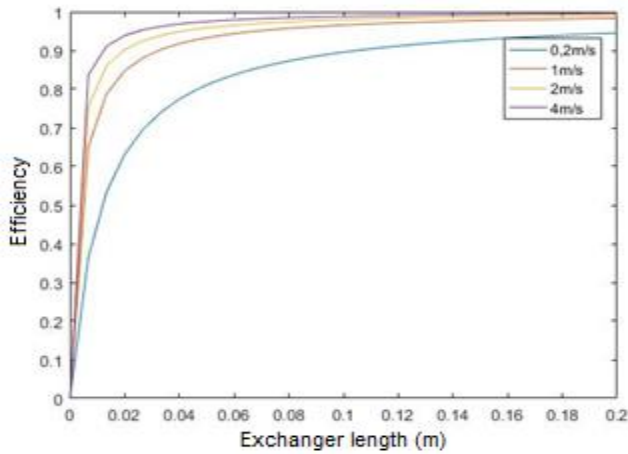


**Figure 9.** Evolution of the thermal efficiency of the exchanger for different inlet air speeds.

## 5. Conclusion

This work focused on a numerical study using the COMSOL Multiphysics software of the hygrothermal transfers which took place in an evaporative exchanger with the aim of cooling the air. This study allowed to note that there is a drop of 14 K along the porous plates of fired clay. Speed has an influence on outlet temperatures and relative humidity. For a speed of 0.2m/s, the temperature variation is 16 K and for speeds ranging from 2 m/s to 4m/s, the temperature variations are approximately 17 K. For gaps in porous plates of fired clay less than 2cm, the thermal efficiency varies 92% to 98%.

## Abbreviations

$M_i$ : Mass of fluid in kg  
 $C_{pi}$ : Specific thermal in  $J.kg^{-1}.K^{-1}$   
 $T_i$ : Temperature of elements i in K  
 $T_j$ : Temperature of elements j in K  
 $h_{xji}$ : Convection transfer coefficient  
 $FSA_i$ : Absorbed solar flow (i) in W  
 $\Delta S$ : Surface variation  
 $R_v$ : water vapor constant  
 $\dot{m}_{ex}$ : Evaporated water debit in kg/h  
 $P_{vsat}$ : Saturation vapor pressure ( $P_a$ )  
 $A_p$ : Water section in  $m^2$   
 $h_a$ : Air convection coefficient in ( $W.m^{-2}.K^{-1}$ )  
 $\lambda_a$ : Thermal conductivity of air ( $W.m^{-1}.K^{-1}$ )  
 $L_c$ : Characteristic length in m.  
 $Re$ : Reynolds number  
 $Pr$ : Prandtl number  
 $\rho$ : Density of the fluid in  $kg/m^3$ ;  
 $\mu$ : Dynamic viscosity in  $kg/(m.s)$  ;  
 $V$ : Velocity in  $m/s$  ;  
 $D_h$ : Hydraulic diameter in m.  
 $K_c$ : Mass transfer coefficient in ( $m.s^{-1}$ )

$D$ : Diffusion coefficient in ( $m^2.s^{-1}$ )

$Sc$ : Number of Schmidt

## Acknowledgments

The International Science Program (ISP) - BUF 01 (Burkina Faso) is acknowledged.

## Disclosure Statement

## Compliance with Ethical Standards

This article does not contain any studies involving human or animal subjects.

## Conflicts of Interest

The authors declare no conflicts of interest

## References

- [1] World Bank Technical (1999): Paper no. 421, Energy Series, Evaporative Air-Conditioning, Applications for Environmentally Friendly Cooling, The International Bank for Reconstruction and Development, The World Bank.
- [2] Rusten, E. (1985) Understanding Evaporative Cooling, Volunteers in Technical Assistance. Technical Paper #35. VITA, Virginia, USA.
- [3] Sushmita, MD, Hemant, D., and Radhacharan, V. (2008) Vegetables in Evaporative Cool Chamber and in Ambient, Macmillan Publi. Ltd., London and Basingstoke, p. 1-10.
- [4] Watt, J. R. (1963) Evaporative air conditioning. New York: The Industrial Press, p. 300.
- [5] Arab M. (2010): 3D stochastic reconstruction of a porous ceramic material from experimental images and evaluation of its thermal conductivity and permeability, Doctoral Thesis, University of Limoges, France.
- [6] Mamoudou M. N. (1989): Theoretical study of a solar hot air generator consisting of an agricultural greenhouse and underground heat storage using conduits. Application to drying, 3rd cycle Doctoral Thesis, Blaise Pascal University (Clermont Ferrand II), France.
- [7] Cerci Y. (2003): A new ideal evaporative freezing cycle, International Journal of Heat and Mass Transfer 46 2967–2974.
- [8] Kaboré B., Kam S., Ouedraogo G. W. P., Zeghmati B., Bathiabo D. J. (2017): Numerical and parametric analysis of vertical input and output parts of an air-soil heat exchanger in the Sahelian zone, International Journal of Research (IJR) 4 (10) 1461-1469.
- [9] Bejan A. (2005): Convection heat transfer, Second Edition, John Wiley Inter-Science Publication.

- [10] Kam S. (2009): Physico-chemical characterization and study of hygrothermal transfers within a material in hot and dry climate, Doctoral thesis, University of Ouagadougou, Burkina Faso.
- [11] Wu J. M., Huang X., Zhang H. (2009): Numerical investigation on the heat and mass transfer in a direct evaporative cooler, *Applied Thermal Engineering* 29, 195-201.
- [12] DISSA A. O. et al (2010): Study of the thermal performance of a local refrigerator based on the evaporation of water through a porous fired clay wall", *Afrique Science* 06(1) 1-12 ISSN 1813-548X.
- [13] Kunzel H. M. (1995): Simultaneous Heat and Moisture Transport in Building Components One- and Two-dimensional Calculation Using Simple Parameters," Rapport, Institut Fraunhofer de physique des b âiments, Allemagne".
- [14] CUCE, Pinar Mert and Saffa R. (2016): A state of the art review of evaporative cooling systems for building applications," *Renewable and Sustainable Energy Reviews*, Vol. 54, pp. 1240-1249.